The Distribution of Gas Molecules at the Diffraction Center in the Electron Diffraction Experiment*

By Yonezo MORINO and Yoshitada MURATA

(Received July 15, 1964)

The mean square amplitude determined by electron diffraction provides us with valuable information regarding the dynamical properties of molecules. Since, however, the values of the mean square amplitudes directly obtained from our measurements are strongly influenced by the delocalization of the sample, physically significant values cannot be obtained unless the correction for this effect is properly made. Moreover, the distribution of gas molecules depends on the shape of the nozzle, and sometimes a systematic error from this origin is introduced into the observed atomic distances.

The effect of a finite sample size has been discussed by Karle and Karle,[1] Harvey et al.,[2] and Kuchitsu.[3] Kuchitsu evaluated the distribution of gas molecules from a gradual decrease in the background curve at more than 80 in the q-scale. His basic idea was that the decrease was produced by the shielding of electron beams by the edge of the nozzle. The principle has been extended in the present experiment for a nozzle with an artificial diaphragm especially designed for the measurement of the distribution of gas molecules.

The Measurement of the Distribution of Gas Molecules at the Diffraction Center

A diaphragm with a circular aperture at its center is attached immediately behind the nozzle. The main electron beam is adjusted to pass through the center of the aperture at a right angle to the plane of the diaphragm, as is shown in Fig. 1. If diffraction occurs in an infinitesimally small region at O, as assumed in the theoretical calculation, the diffraction intensity on the plate should be cut off sharply at point P, with no blackening beyond that point. However, as the gas stream has a finite width, some electrons diffracted at points nearer to the plate than O arrive at points farther away than P, resulting in a gradual change in the intensity. From the measurement of the change in the intensity near point P on the photograph, information is obtained regarding the distribution function, $f(x)$.

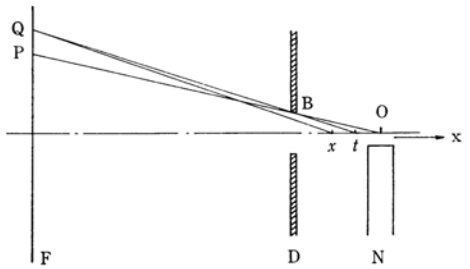

Fig. 1. Schematic representation of the arrangement for measurement of the gas distribution.
N: Nozzle D: Circular diaphragm
F: Photographic plate

If multiple scattering is ignored, the scattered intensities with and without the diaphragm, $I_T{}^a$ and $I_T{}^b$ respectively, are given by the following expressions:

$$P(t)=\frac{I_T{}^a(s_0)}{I_T{}^b(s_0)}=\frac{\int_{-\infty}^{t} I_T(x, s_0)f(x)\mathrm{d}x}{\int_{-\infty}^{\infty} I_T(x, s_0)f(x)\mathrm{d}x} \qquad (1)$$

where $I_T(x, s_0)$ denotes the total intensity scattered at point x along the main beam toward point Q, which corresponds to the direction, s_0, from the origin. The origin of the x axis is taken at a point above the center of the nozzle, while the negative direction of the x axis is taken from the nozzle towards the photographic plate. The function $f(x)$ denotes the linear density of gas molecules along the path of the primary electron beam. The upper limit of Eq. 1, t, designates the point at which line QB intersects the x axis, B being the edge of the diaphragm. The electrons diffracted before reaching point t hit the diaphragm and do not arrive at the photographic plate.

When the main portion of the gaseous sample is localized in a small region near point O, $f(x)$ decreases steeply as x increases. In such a case, $I(x, s_0)$ is supposed to be nearly constant in the range where $f(x)$ is of a significant magnitude, and Eq. 1 is simply

* Some preliminary results of this work were presented at the International Conference on Magnetism and Crystallography, Kyoto, 1961.

1) I. L. Karle and J. Karle, *J. Chem. Phys.*, **18**, 963 (1950).
2) R. B. Harvey, F. A. Keidel and S. H. Bauer, *J. Appl. Phys.*, **21**, 860 (1950).
3) K. Kuchitsu, This Bulletin, **32**, 748 (1959).

approximated by:

$$P(t)=\int_{-\infty}^{t} f(x)\mathrm{d}x \qquad (2)$$

when $f(x)$ is normalized as:

$$\int_{-\infty}^{\infty} f(x)\mathrm{d}x=1 \qquad (3)$$

The accuracy of such an approximation will be considered in Appendix II.

A diaphragm with an aperture 2.38 mm. in diameter was attached to the nozzle at a distance of 4.51 mm. The primary beam passed 0.41 mm. above the top of the nozzle. The surface of the diaphragm was coated with colloidal graphite powder in order to decrease the extraneous scattering.

A set of three photographs was taken by using silicon tetrachloride. The first photograph was taken for a blank test to make a correction for the extraneous scattering. The second was taken with the diaphragm, and the third, without it. The experimental conditions were the same as those in the case of the needle-type nozzle described in a previous paper.[4] The microphotometer tracings shown in Fig. 2 clearly indicate the decrease in

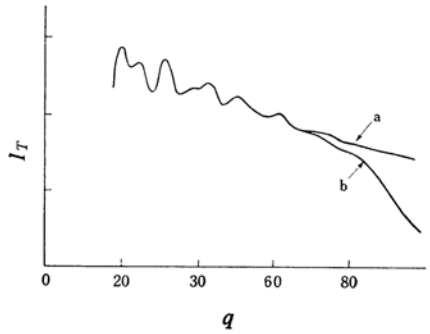

Fig. 2. Photometer curves of $SiCl_4$ with and without the diaphragm. The ordinate scale is in arbitrary units.
a: Without the diaphragm
b: With the diaphragm

intensity when the diaphragm was used. By the use of the dimension of the diaphragm and the observed ratio of the diffraction intensities at s_0, the function of t, $P(t)$, in Eq. 2 was derived. The $P(t)$ curve is shown in Fig. 3. The fact that the $P(t)$ curve was 1/2 at $t=0$ is consistent with the expectation derived from the assumption that the distribution of gas molecules is symmetric across the origin. It also indicates that the experimental arrangement conformed to our original plan. The plot of $\log(1-P(t))$ against t was found to be closely approximated by two straight lines, as is shown in Fig. 4. It was

4) Y. Morino and Y. Murata, This Bulletin, 38, 105 (1965).

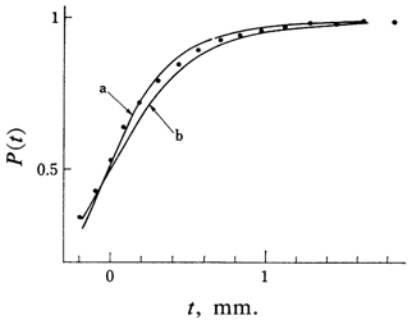

Fig. 3. Observed and calculated $P(t)$ curves. Observed values are shown in dots.
a: Calculated curve obtained by Eq. 9
b: Calculated curve obtained by Eq. 10

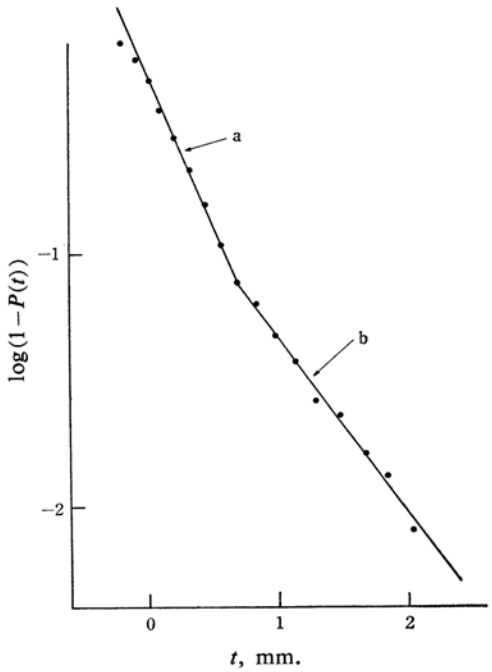

Fig. 4. Plots of $\log(1-P(t))$ vs. t; observed values are shown in dots. The straight lines a and b are represented by Eqs. 4a and 4b respectively. A break at $t=0.7$ is of little significance, since the lines a and b are only approximate representations of the original curve, which may lie on a smooth line. See descriptions in the text.

found that:

for

$$0.7 \geqq t \geqq 0, \quad P(t)=1-\frac{1}{2}\exp(-2.74t) \qquad (4a)$$

and for

$$t \geqq 0.7, \qquad P(t)=1-0.224\exp(-1.59t) \qquad (4b)$$

when t was measured in millimeter. By differentiating the above equations by t, the distribution function on the beam is represented

by:

for $0.7 \geqq x \geqq 0$,

$$f(x) = (2.74/2)\exp(-2.74x) \quad (5a)$$

and for $x \geqq 0.7$,

$$f(x) = 0.356\exp(-1.59x) \quad (5b)$$

where x is also measured in millimeter. It may be possible to assume the same distribution function on the negative side of the x axis, because the value of $P(t)$ at $t=0$ was compatible with the assumption of the symmetric distribution around the origin. It seems strange that the density functions obtained above, 5a and 5b, are discontinuous at the intersection $x=0.7$. The sharp break results from the approximation that $\log(1-P(t))$ may be expressed by two straight lines.

As will be shown in Appendix I, the atomic distances and the index of resolution are little affected by the finite spread of gas molecules at the diffraction center, whereas the apparent increment in the root-mean-square amplitude, Δl, is given by:

$$\Delta l_{ij} = r_{ij}^2 / l_{ij}\rho^2 L_0^2 \quad (6)$$

if the distribution function $f(x) = (\rho/2) \times \exp(-\rho|x|)$, with $\rho = 2.74\,\mathrm{mm}^{-1}$, is used through the whole range. The calculated values are listed in column a in Table I. In the range of $|x| \geqq 0.7$, the real distribution is slightly different from this function; it is expressed by another exponential function, 5b, which results in a 10% increase in the increment. The values of Δl derived with this function are shown in column b of Table I.

TABLE I. CORRECTION FOR THE MEAN AMPLITUDES DUE TO THE FINITE SPREAD OF GAS MOLECULES (in Å units)

	l_a(obs)	$\Delta l(a)$	$\Delta l(b)$
Si-Cl	0.0479	0.0008	0.0009
Cl-Cl	0.0905	0.0012	0.0013

$\Delta l(a)$: Calculated by Eq. 6, on the assumption that the gas distritution is expressed by a simple distribution function 5a.
$\Delta l(b)$: Calculated by taking both functions 5a and 5b into account.

In the calculations described above, several approximations and assumptions were made. We will consider the validity of these approximations and assumptions below.

First, the assumption that the main portion of the gaseous molecules is confined to the range $|x/L_0| \ll 1$ is satisfied, because the value of $f(x)$ at $L_0 = 118$ mm. is very small, as is evident from Eq. 5. Next, the multiple scattering[5] can be disregarded in this experiment, because the indices of resolution were found to be unity or at least very close to unity.[4] This means that no "delocalization" of the gas molecules in the camera box[6] was recognized.

It will be shown in Appendix II that the approximation made in Eq. 2 is valid within 5% if we consider that t is less than 2 mm. and $L_0 = 118$ mm.

The Flow of Gas Molecules Emitted from the Nozzle

It is interesting to see what kind of gas flow is responsible for the distribution of gas molecules obtained above. The model to be considered first is the simplest one, in which the gas molecules are emitted from the center of the nozzle with an equal probability in all directions. The solid angle, $d\omega$, which corresponds to a rectangular area enclosed by the width, d, and the length of dx on the beam is given by:

$$d\omega = ad\,dx/(x^2+a^2)^{3/2} \quad (7)$$

where a is the distance from the top of the nozzle to the main beam ($a=0.41$ mm.). Therefore, the normalized distribution function is represented by:

$$f(x) = a^2/2(x^2+a^2)^{3/2} \quad (8)$$

It follows that:

$$P(t) = (1/2)\,(1+t/(a^2+t^2)^{1/2}) \quad (9)$$

This formula, which denotes the integrated distribution of the gas molecules, contains only a measurable parameter, a. In Fig. 3, curve a shows the $P(t)$ which was obtained by inserting the actual dimension of $a=0.41$ mm. into Eq. 9.

In the model described above, the drastic assumption was made that the flow of the molecules comes from a single point, i. e., from the center of the top of the nozzle. In the actual experiment, however, the molecules come out from the whole area of the nozzle exit. It is, accordingly, likely that the gas distribution near the nozzle is quite different from that derived above. Thus another model must be considered, one in which gas molecules are emitted from the entire opening of the nozzle with an equal probability in every direction. It is easy to show that, when the radius of the nozzle is b, the distribution function on the main beam is given by:

$$f(x) = \int_0^b \int_0^{2\pi} \frac{Aar\,dr\,d\theta}{(x^2+a^2+r^2-2xr\cos\theta)^{3/2}} \quad (10)$$

5) J. A. Hoerni, *Phys. Rev.*, **102**, 1530 (1956).

6) L. S. Bartell, *J. Appl. Phys.*, **31**, 252 (1960).

where A is a normalization constant.

An approximate calculation was carried out by the use of a series expansion, instead of exact integration using the elliptic function of the second kind. The results are shown by curve b in Fig. 3. Both of the calculated $P(t)$ functions, a and b, are consistent with the observed $P(t)$, but a detailed comparison reveals that the first model is slightly better than the second. It may be considered from this finding that the gas flows faster in the central part than in the outer part of the nozzle; in other words, the flow is more or less viscous within the tube, even though the stream of gas molecules behaves as a molecular flow after leaving the nozzle. In fact, the mean free path in the nozzle is estimated to be 0.03 mm., much smaller than the diameter of the nozzle, 0.55 mm.

The Effect of Asymmetric Distribution at the Nozzle

It was shown in the previous section that, in the case of the needle-type nozzle, the gas distribution has its center exactly over the nozzle and fades away symmetrically from the center in both directions. However, in the case of the drum-type nozzle, as is shown in Fig. 8 of Ref. 3, the distribution may be asymmetric with respect to the center of the nozzle, because the front edge of the nozzle was cut off in a cone-shape in order to secure a wide angle for the diffracted electrons. Hence, it is worthwhile measuring the difference in the distribution on both sides and estimating its influence on the observed molecular parameters.

For the needle-type nozzle, it was found in this study that the distribution may be represented by an exponential function, $C\exp(-\rho|x|)$. However, in the case of the drum-type nozzle, a Gaussian function is more suitable for the distribution. This is because the emitted gas molecules hit the upper wall of the nozzle and recoil to give an increased gas density near the center of the nozzle and an increased spread of the gas distribution. Accordingly, for a drum-type nozzle, the distribution may be fitted by two Gaussian functions with different parameters in the exponents, one for the positive side and the other for the negative side. It may be reasonable to take the maximum at $x=0$. Thus the distribution function in the regular orientation is assumed to be

$$f(x)=C_1\exp(-ax^2), \quad \text{for} \quad x>0 \tag{11a}$$

and

$$f(x)=C_2\exp(-bx^2), \quad \text{for} \quad x<0 \tag{11b}$$

If the functions are taken to be continuous at $x=0$ and are normalized to unity, then the coefficient is given by:

$$C_1=C_2=2(a/\pi)^{1/2}/(1+K) \tag{12}$$

where $K=(a/b)^{1/2}$ denotes the ratio of the half-widths. In order to estimate parameters a and b, two photographs were taken, one at the regular orientation to obtain the constant b, and the other at the reversed orientation of the nozzle, i. e., by turning the other face of the nozzle to the plate, to obtain the constant a. Silicon tetrachloride was taken as a sample, and experimental conditions were chosen to be almost the same as in the case of the drum-type nozzle described in the previous paper.[4] For both regular and reversed orientations of the nozzle, the experimental background curves were compared with the theoretical curve.[3]

The observed $P(t)$ curve should fit with

$$P(t)=\frac{K}{1+K}+\frac{1}{1+K}\,\mathrm{Erf}(\sqrt{a}\,t) \tag{13a}$$

for the regular position, and

$$P(t)=\frac{1}{1+K}+\frac{K}{1+K}\,\mathrm{Erf}(\sqrt{b}\,t) \tag{13b}$$

for the reversed orientation. Parameters a and b cannot be determined separately, because both Eqs. 13a and 13b contain K, in addition to a single parameter, a or b. Hence, by considering both curves simultaneously, the values of a and b were obtained to be $a=0.42\,\mathrm{mm}^{-2}$ and $b=0.67\,\mathrm{mm}^{-2}$, while $K=0.79$. It is interesting to notice that 0.79 is much larger than the value presumed from the geometrical dimension of the nozzle; if we assume that the half-width of each side of the distribution is proportional to the width of the nozzle wall, K should be 0.53. The result indicates that the asymmetry of the gas distribution is smaller than the geometrical asymmetry of the nozzle.

As will be shown in Appendix I, the apparent increases in the atomic distances and in the root-mean-square amplitudes are given by:

$$\frac{\Delta r}{r}=-\frac{1-K}{\sqrt{\pi a}\,L_0} \tag{14}$$

and:

$$\frac{\Delta l}{l}=\frac{(1-K+K^2)}{4aL_0^2}\left(\frac{r}{l}\right)^2 \tag{15}$$

The values of a and b determined above lead to the result that Δr's are -0.0032 Å and -0.0052 Å, while Δl's are 0.0031 Å and 0.0045 Å for Si–Cl and Cl–Cl respectively.

On the other hand, a small discrepancy in the atomic distance was observed by reversing the orientation of the nozzle, as has been described in a previous paper.[4] Since the observed differences in the atomic distances, shown in Table I of Ref. 4, correspond to $2\Delta r$, the apparent increases, Δr caused by the asymmetric distribution are shown to be -0.0022 Å

for Si–Cl and −0.0035 Å for Cl–Cl; they are in good agreement with the values obtained above by estimating the gas distribution.

It should be noted that the apparent increase in the mean amplitudes is much larger in the case of the drum-type nozzle than in the case of the needle-type nozzle. The mean amplitudes obtained by the drum-type nozzle, when corrected for the gas distribution given above, agree well with the values obtained by the needle-type nozzle, as Table II shows.

TABLE II. MEAN AMPLITUDES OBTAINED BY TWO TYPES OF NOZZLES (in Å units)

		l(Si–Cl)	l(Cl–Cl)
Needle-type	(a)	0.0479	0.0905
	(b)	0.0470±0.0016	0.0892±0.0024
Drum-type (regular orientation)	(a)	0.0495	0.0943
	(b)	0.0464±0.0045	0.0898±0.0053

(a): Most probable values obtained by the method of least squares to each of four photographs.
(b): Final values. The errors associated with the drum-type nozzle caused by the estimation of the finite sample size were assumed to be 100% of the corrections.

Summary

A method has been proposed for estimating the distribution of gas molecules at the diffraction center in order to evaluate the correction for finite sample size in gas electron diffraction. The distribution measured in this way has been interpreted by a simple model regarding the motion of the gas molecules in the vicinity of the nozzle. A slight asymmetry of the nozzle construction produces in the atomic distances a deviation which cannot be disregarded if an accurate measurement is desired.

The expenses of the work were defrayed by a grant from the Ministry of Education, to which the authors' thanks are due.

Department of Chemistry
Faculty of Science
The University of Tokyo
Hongo, Tokyo

Appendix I

Let us consider the influence of the finite distribution of gas molecules at the diffraction center upon the atomic distances, mean square amplitudes, and index of resolution.

If the gas distribution is given by $f(x)$, the observed total intensity is expressed by:

$$I_T(s_0)=\int_{-\infty}^{\infty} I_T(x,s_0)f(x)\,dx \tag{A1}$$

and the observed molecular intensity function is given by:

$$M(s_0)=\int_{-\infty}^{\infty} I_M(x,s_0)f(x)\,dx \Big/ \int_{-\infty}^{\infty} I_B(x,s_0)f(x)\,dx \tag{A2}$$

where $I_M(x,s_0)$ and $I_B(x,s_0)$ are the functions of x through s and L:

$$I_M(x,s_0)=\sum_{ij} C_{ij}\frac{L}{(L^2+R^2)^{3/2}s^4}\frac{\sin sr_{ij}}{sr_{ij}} \times\exp(-\alpha_{ij}s^2) \tag{A3}$$

and $$I_B(x,s_0)=\sum_{ij} C'_{ij}\frac{L}{(L^2+R^2)^{3/2}s^4} \tag{A4}$$

To the second order of approximation with regard to $z=x/L_0$ and $a^2=(R/L_0)^2$ (L_0 being the camera length from the origin of the x axis, and R, the radius of point P on the photographic plate), s is given by:

$$s=s_0(1-\gamma z+\delta z^2) \tag{A5}$$

where $$\gamma=1-\frac{3}{4}bs_0^2+\frac{1}{8}b^2s_0^4 \tag{A6}$$

$$\delta=1-\frac{15}{8}bs_0^2+\frac{41}{32}b^2s_0^4 \tag{A7}$$

and $$L=L_0+x \tag{A8}$$

$$a^2=bs_0^2\left(1+\frac{3}{4}bs_0^2\right) \tag{A9}$$

Here s_0 denotes the s-value for the diffraction at the origin to point P and $b=\lambda^2/4\pi^2$. Expanding Eqs. A3 and A4 in terms of x and a^2, and disregarding coefficients smaller than 1% of the largest one, it can be shown that:

$$\begin{aligned}M(s)=&\sum I_M(0,s_0)\Big[(1+\langle z\rangle+2\langle z^2\rangle-2\langle z\rangle^2)\\&+\left(2\alpha\langle z\rangle-\frac{1}{2}r^2\langle z^2\rangle\right)s_0^2\\&+\left\{-\frac{3}{2}\alpha b\langle z\rangle+\left(\frac{3}{4}br^2+2\alpha^2\right)\langle z^2\rangle\right\}s_0^4\Big]\\&+\sum I_M(0,s_0)\frac{\cos s_0r}{\sin s_0r}rs_0\Big[(-\langle z\rangle-2\langle z^2\rangle+2\langle z\rangle^2)\\&+\left(\frac{3}{4}b\langle z\rangle-2\alpha\langle z^2\rangle\right)s_0^2\\&+\left(-\frac{1}{8}b^2\langle z\rangle+3\alpha b\langle z^2\rangle\right)s_0^4\Big]\end{aligned} \tag{A10}$$

where $$\langle z\rangle=\int_{-\infty}^{\infty} zf(x)\,dx \tag{A11}$$

On the other hand, if it is assumed that the diffraction intensity can be expressed by the usual diffraction formula with slightly modified molecular parameters:

$$M(s)=\sum kC\exp(-(\alpha+\Delta\alpha)s_0^2)\sin(s_0r+s_0\Delta r)/ s_0(r+\Delta r) \tag{A12}$$

a formula corresponding to Eq. A10 is obtained by expanding Eq. A12 with regard to the small quantities. Comparing the corresponding terms in s_0, the following relations are obtained:

$$1+\langle z\rangle+2\langle z^2\rangle-2\langle z\rangle^2=k(1-\Delta r/r) \tag{A13}$$

$$2\alpha\langle z\rangle-\frac{1}{2}r^2\langle z^2\rangle=-k(1-\Delta r/r)(\Delta\alpha+\Delta r^2/2) \quad \text{(A14)}$$

$$(3b/4)(-2\alpha\langle z\rangle+r^2\langle z^2\rangle)=k(1-\Delta r/r)\times(\Delta\alpha\Delta r^2/2+\Delta\alpha^2/2+\Delta r^4/4!) \quad \text{(A15)}$$

$$-r(\langle z\rangle+2\langle z^2\rangle-2\langle z\rangle^2)=k(1-\Delta r/r)\Delta r \quad \text{(A16)}$$

$$-r(2\alpha\langle z^2\rangle-\frac{3}{4}b\langle z\rangle)=-k(\Delta\alpha+\Delta r^2/6)(1-\Delta r/r)\Delta r \quad \text{(A17)}$$

and

$$r(3\alpha b\langle z^2\rangle-\frac{1}{8}b^2\langle z\rangle)=k(1-\Delta r/r)\Delta r\times(\Delta\alpha\Delta r^2/6+\Delta\alpha^2/2+\Delta r^4/5!) \quad \text{(A18)}$$

From Eqs. A13 and A16 we obtain:

$$\Delta r/r=-(\langle z\rangle+2\langle z^2\rangle-3\langle z\rangle^2) \quad \text{(A19)}$$

By inserting the result in Eq. A13, it is shown that:

$$k=1 \quad \text{(A20)}$$

and also in Eq. A14:

$$\Delta\alpha=\frac{1}{2}r^2\langle z^2\rangle-2\alpha\langle z\rangle-\frac{1}{2}r^2\langle z\rangle^2+2\alpha\langle z\rangle^2 \quad \text{(A21)}$$

(I) The Case of a Symmetric Distribution.—It was found that the distribution of gas molecules for the needle-type nozzle was symmetrical with respect to the origin $x=0$. In this case, $\langle z\rangle=0$, and Eqs. A19 and A21 are simplified as follows:

$$\Delta r/r=-2\langle z^2\rangle \quad \text{(A22)}$$

and

$$\Delta\alpha=\frac{1}{2}r^2\langle z^2\rangle \quad \text{(A23)}$$

Now, if the distribution function obtained above, $f(x)=(\rho/2)\exp(-\rho|x|)$, with $\rho=2.74\,\mathrm{mm}^{-1}$, is used over the whole range, the mean value of z^2 is given by:

$$\langle z^2\rangle=2/\rho^2L_0^2 \quad \text{(A24)}$$

and: $$\Delta r/r=-4/\rho^2L_0^2 \quad \text{(A25)}$$

The apparent increase in the mean amplitude is thus obtained by:

$$\Delta l=\Delta\alpha/l=r^2/l\rho^2L_0^2 \quad \text{(A26)}$$

(II) The Case of Asymmetric Distribution.—For the drum-type nozzle, we have evidence that the distribution of gas molecules is not symmetrical with respect to the origin. Therefore, correction must be made in such a case.

If the distribution function in the regular orientation is expressed by the following formulas:

$$f(x)=C\exp(-ax^2) \quad \text{for } x>0 \quad \text{(A27)}$$

and $$f(x)=C\exp(-bx^2) \quad \text{for } x<0 \quad \text{(A28)}$$

where $$C=2\sqrt{a}/\sqrt{\pi}\,(1+K) \quad \text{(A29)}$$

and $$K^2=a/b \quad \text{(A30)}$$

the means of z and z^2 are expressed by:

$$\langle z\rangle=(1-K)/\sqrt{\pi a}\,L_0 \quad \text{(A31)}$$

and $$\langle z^2\rangle=(1-K+K^2)/2aL_0^2 \quad \text{(A32)}$$

The observed values of $a=0.418$, $K=0.787$ and $L_0=118$ lead to the results $\langle z\rangle=1.57\times10^{-3}$, and $\langle z^2\rangle=7.15\times10^{-5}$. Therefore, disregarding smaller terms, Eqs. A19 and A21 reduce to:

$$\Delta r/r=(K-1)/\sqrt{\pi a}\,L_0 \quad \text{(A33)}$$

and $$\Delta\alpha=(1-K+K^2)r^2/4aL_0^2 \quad \text{(A34)}$$

and $$\Delta l/l=(1-K+K^2)r^2/4l^2aL_0^2 \quad \text{(A35)}$$

Equations A15, A17 and A18 give further relations among Δr, $\Delta\alpha$ and k, but they are not always reasonable, because the basic assumption A12 does not hold exactly for such higher terms.

Appendix II

It will be worthwhile to consider the uncertainty of the approximation used in Eq. 2; that is:

$$P(t)=\frac{\int_{-\infty}^{t}I_Tf(x)\,dx}{\int_{-\infty}^{\infty}I_Tf(x)\,dx}=\int_{-\infty}^{t}f(x)\,dx \quad \text{(A36)}$$

Now the total scattering intensity is given by:

$$I_T=I_B(1+M) \quad \text{(A37)}$$

By expanding it in terms of z,

$$I_T\cong I_T{}^0(1+2z+z^2)+I_B{}^0\times\left[\left(\frac{dM}{dz}\right)_0z+2\left(\frac{dM}{dz}\right)_0z^2+\frac{1}{2}\left(\frac{d^2M}{dz^2}\right)_0z^2\right] \quad \text{(A38)}$$

while by assuming the symmetric distribution $f(x)=(\rho/2)\exp(-\rho|x|)$, the $P(t)$ function is shown to be as follows:

$$P(t)=\int_{-\infty}^{t}f(x)\,dx(1+\Delta) \quad \text{(A39)}$$

where

$$\Delta=\frac{1}{L_0}\left(t-\frac{1}{\rho}\right)\left[2I_T{}^0+I_B{}^0\left(\frac{dM}{dz}\right)_0\right]\Big/\int_{-\infty}^{\infty}I_Tf(x)\,dx \quad \text{(A40)}$$

By considering the fact that:

$$2/\rho^2L_0^2=2\times10^{-5}\ll1$$

$$I_B{}^0\cong I_T{}^0$$

$$\left|\left(\frac{dM}{dz}\right)_0\right|\cong1$$

$$\left|I_B{}^0\left(\frac{dM}{dz}\right)_0\frac{1}{\rho^2L_0^2}\right|\ll I_T{}^0$$

$$\left|\left(\frac{d^2M}{dz^2}\right)_0\right|<(rs_0+4\alpha s_0^2)$$

$$\left|I_B{}^0\left(\frac{d^2M}{dz^2}\right)_0\frac{1}{\rho^2L_0^2}\right|<\frac{1}{100}I_T{}^0$$

and that, therefore:

$$\int_{-\infty}^{\infty}I_Tf(x)\,dx\cong I_T{}^0$$

Eq. A40 may be roughly evaluated as follows:

$$|\Delta|\cong\frac{2}{L_0}\left(t-\frac{1}{\rho}\right)\left(1+\frac{1}{2}\right)=\frac{3}{L_0}\left(t-\frac{1}{\rho}\right)\cong5\% \quad \text{(A41)}$$

In conclusion, the approximation made in Eq. 2 is satisfied within an uncertainty of 5%.